On the origin of long secondary periods in semi-regular variables

E.A. Olivier and P.R. Wood

Research School of Astronomy and Astrophysics, Australian National University, Cotter Road, Weston Creek ACT 2611, Australia

ABSTRACT

The presence of a long secondary period (LSP) in the light-curves of some local semi-regular variables has been known for many years. Furthermore, the LSPs have recently been found in the light curves of approximately 25% of semi-regular variables in the LMC. They typically have a length ∼500–4000 days, some 5–15 times longer than the primary period. Binarity, pulsation, periodic dust ejection and rotation have been suggested as the origin of the LSPs. Here we analyse echelle spectra of a group of local semi-regular variables with LSPs (henceforth LSPVs) in order to try to distinguish between these suggestions. In general, we find that LSPVs do not have broader spectral features than semi-regulars without a long secondary period (henceforth non-LSPVs). The general upper limit on the equatorial rotation velocity of 3 km/s rules out rotating spot and similar models. One LSPV, V Hya, does have broader spectral lines than similar carbon stars, but it is shown here that rotation alone is not a good model for explaining the broad lines. Mid-infrared colours of LSPs and non-LSPVs are similar and there are no LSPVs showing the large [60] – [25] IRAS colour exhibited by some RCB stars. Thus there is no evidence for periodic dust ejection from LSPVs. Finally, we find that the LSPVs show larger radial velocity variations than non-LSPVs, which suggests that LSPs are caused either by binarity or by pulsation. A similar conclusion was derived by Hinkle et al. (2002).

Subject headings:

1. Introduction

It has been known for a long time that some local semi-regular variables show the presence of a long secondary period in their light-curves, typically 5-15 times longer than the primary pulsation period (Houk 1963). Houk (1963) lists 103 such local semi-regular variables while Kiss et al. (1999) list some further objects and show examples of light curves. Recently, Wood et al. (1999), henceforth W99, studied a group of red-variables in the LMC using MACHO data and discovered that about $\sim 25\,\%$ of them show a long secondary periodic variation.

Possible explanations for the LSPs include pulsation, rotation combined with surface irregularities, binary companions and episodic dust ejection (see W99 and Wood 2000a). There is some evidence in favour of each of these suggestions. (1) W99 noted that the period-luminosity relation they saw could be explained by the AGB star being in a semi-detached binary system. In this scenario the AGB variable fills it Roche-lobe, losing mass to its companion. This forms a dusty cloud of matter around the companion, which then obscures the star each time it crosses the line of sight. (2) Barnbaum et al. (1995) found evidence for spectral broadening in V Hya, a known local LSPV, and attributed this to rapid rotation. The rotation velocity ($\sim$ 6-16 km s^{-1}) seem to vary with the same period as the pulsation. They suggested that the LSP of V Hya of about 6200 days could be attributed to a coupling of the radial pulsation (530 day period) with rotation. (3) Olivier et al. (2001) showed V Hya to be reddened during the LSP variations. The LSP amplitudes are 2.4, 2.1, 1.7 and 0.7 mag at J, H, K and L, respectively, while the V amplitude is ~ 3.5 mag (Knapp et al. 1999). It is not clear why the interaction suggested by Barnbaum et al., would give rise to the observed reddening, while the reddening could easily follow from the scenario presented by W99, or from episodic dust ejection in events of the type found by Winters et al. (1994) and Höfner et al. (1995). (4) The presence of large star spots on the surface of AGB stars has been suggested by Schwarzschild (1975), the cool regions being associated with very large convective elements. Recently, the presence of cool magnetic spots on AGB stars has been proposed (see e.g. Soker & Clayton 1999). Combined with rotation, such spots could explain the LSPs: a typical AGB star with a radius of $300\,R_\odot$ and a rotation velocity of 10 km s^{-1} (about one third the break-up velocity) with a large star spot, will give rise to a secondary period of ~ 1500 days.

We note that the rotation velocities of ~ 10 km s^{-1} mentioned above cannot easily be explained as rotation inherited from the main-sequence phase. A one solar mass progenitor rotating at break-up velocity on the main-sequence will give rise to a $300\,R_\odot$ AGB star rotating at only ~ 1 km s^{-1}. It is therefore necessary to invoke binary mass and angular momentum transfer, probably a binary merger, in order to get rotation velocities larger than ~ 1 km s^{-1}. For example, a binary system with each member having a mass of $1.2\,M_\odot$ and a separation of $150\,R_\odot$ which merges to a single star of radius $300\,R_\odot$ (conserving mass and angular momentum) will rotate with a period of ~ 900 days and equatorial surface rotation velocity of ~ 17 km s^{-1}.

In this paper, we examine high resolution spectra of a sample of LSPVs and a similar sample of non-LSPVs in order to look for evidence of rotation and/or radial velocity variations due to binary motion or pulsation. The spectra are part of an on-going monitoring program for these stars. We also examine IRAS data for the sample in order to look for evidence for the dust that might be expected around LSPVs in some of the scenarios listed above.

2. Sample and Observations

A sample of 26 local LSPVs, 9 C-type and 15 M-type, were selected from the list of Houk (1963) for observing. These are listed in Table 1 together with spectral and variable type, primary pulsation period and LSP. Table 2 list the same data for a similar, control group of 30 semi-regulars, 20 M-type and 10 C-type, showing no LSP, selected from the General Catalogue of Variable Stars (GCVS, Kholopov 1985) to be in the same part of the sky as the LSPVs. As can be seen from Tables 1 and 2, pulsation periods range from $\sim 50 - 300$ days and LSPs from $\sim 500 - 4000$ days (excluding V Hya). The Kolmogorov-Smirnov (KS) two-sample test gives a probability of 70% that both samples came from the same parent population in pulsation period i.e. no significant differences in pulsation period exists between the two groups.

Here we examine echelle spectra obtained for the objects listed in Tables 1 and 2 during nine nights over a period of about one year. The spectra were taken with the Coude Echelle spectrograph (31 line/mm echelle grating) on the 74″ telescope at Mount Stromlo Observatory. The detector was a SITe 2048×4096 CCD with 15 micron pixels. The dispersion of the spectra is 1.52 km s^{-1} pixel^{-1}, with a central wavelength of 6563Å(Hα). The resolution is typically 2.75 pixels. Not all objects were observed with the same frequency, in particular only 17 of the non-LSPVs were observed on more than one night. In total 132 high resolution echelle spectra were obtained.

The data were reduced with the *IRAF* software package. The raw images were bias subtracted and any bad-pixels on the CCD were fixed, using standard CCD reduction procedures in *IRAF*. The images were then flat fielded and the wavelength calibrated spectra were extracted using the *IRAF* task *DOECSLIT*. Figure 1 show examples of typical M-type and C-type stellar spectra obtained.

3. Spectral line broadening and rotation

As mentioned earlier, Barnbaum et al (1995) found evidence for spectral broadening in the LSPV V Hya, by comparing its spectrum to that of several other similar carbon stars, in particular U Hya, and suggested the difference might be due to rotation. Figure 2 shows the fourier power spectra of V Hya and U Hya. The power spectrum of U Hya broadened with a line-of-sight rotation velocity of 8 km s^{-1} and limb-darkening coefficient of 0.8 is also shown in Figure 2 (the broadening was done according to the rotational broadening model described in Gray 1976). This power spectrum seem to fit the power spectrum of V Hya fairly well over lower frequencies ($\sim 0 - 2$ cycles/Å) but at higher frequencies ($\sim 2.5 - 4$ cycles/Å) the fit is not good i.e. rotation alone is not a good model for the broadening seen in V Hya. A macro-turbulence model, with the turbulent elements having different radial and tangential velocity distributions, may lead to a better fit. Such a model will have more power at higher frequencies than a simple rotation model (see e.g. Figure 18-9 in Gray 1976).

All stars in our sample have been examined for the presence of broadening caused by rotation. The M-type stars were divided into 3 groups, according to a spectral type index, R, which is simply the ratio of the flux in a 10 Å waveband shortward and longward of the TiO bandhead at 7050 Å. Power spectra calculated from the flux spectra (all stars at different dates), with a noise to power ratio at 2 cycles/Å of less than ∼5% are shown in Figure 3. The spectra are grouped by spectral type.

The main effect of rotation on the power spectrum is to alter the overall slope (as seen in Fig. 2). In order to estimate the slope, a simple curve of the form $Log(p) = const. - \alpha\,\sigma^2$ (where p is the power and σ is in cycles/Å) was fitted to each power spectrum in Figure 3, with α thus being an indicator of the slope. The fitting were done by least-squares minimization over the range $0.4 - 3.5$ cycles/Å. Figure 4 shows the mean values of α for each group. Also shown is the student t-test statistic t and the associated probability, p_t, that the values of α for non-LSPVs and LSPVs are drawn from distributions with the same mean. It is clear there is no significant difference in $\bar{\alpha}$ for LSPVs and non-LSPVs for groups 3 and 4. The differences for groups 1 and 2 are significant at the 5% level, with the non-LSPVs power spectra having a *steeper* slope than the LSPVs, in the mean. Within the context of the rotation model, this would suggest *less* rotation in LSPVs than non-LSPVs, certainly not in agreement with the suggestion that the LSPs may originate from rotation. In general, looking at Figure 4, it seems that the LSPVs in groups 1 and 2 have more power at higher frequencies (3-4 cycles/Å) than the corresponding non-LSPVs. This suggests that the LSP phenomenon in some way decreases line broadening. Possibilities include a reduction in the pulsation velocity or velocity gradient in the stellar atmosphere, or more prominent lines from the cooler parts of the photosphere where thermal broadening is less.

To quantify the limits the present results put on the rotation in LSPVs, we note by examining Figure 4, that a 2-sigma uncertainty in $\bar{\alpha}$ correspond to 0.02. The rotation model of Gray shows that a 3.0 km/s equatorial rotation velocity would increase $\bar{\alpha}$ by 0.02 (a 5 km/s velocity would increase $\bar{\alpha}$ by 0.06). Given the actual observed *decrease* in $\bar{\alpha}$, we can very conservatively rule out rotation velocities greater than 3 km/s as a general characteristic of LSPVs.

Given that these stars have radii of $\sim 170\,R_{\odot}$, a 3 km/s rotation velocity would give a rotation period of 2868 days. Since only 4 of the 28 LSPVs here have secondary periods longer than 2868 days, the rotation period can not generally be equated to the LSP. This rules out rotating spot models for the LSPVs. Even rotating stars of dipolar shape (whose observed period would be half the rotation period) are ruled out in most cases as well.

4. Radial velocity variations

The large number of molecular absorption lines present in the spectra of these late type stars make it possible to determine very accurate relative radial velocities via cross-correlation. Heliocentric velocities were calculated for each star on multiple dates. Then the velocity changes v_r' relative to a specific date were computed for each star. The velocity changes were calculated using order 80 ($\sim$7020Å$-$7160Å). Other orders (wavelength ranges) were used as well to cross check, and these velocities agreed to better than 0.3 km s^{-1}. The velocity changes that occurred for each star are shown as a histogram in Figure 5, with separate histograms for the LSPV and non-LSPV groups.

It is clear that the distribution of LSPV velocity changes is broader than that of the non-LSPVs. The KS two-sample test gives a probability that the two distributions came from the same parent population of less than 0.02 i.e. the two distributions are significantly different. Note that the width of the non-LSPV histogram is a measure of the pulsation velocity associated with the pulsation in these SR variables: the LSVP histogram width will have a pulsation component similar to that of the non-LSPV histogram. The larger velocity changes in the LSPVs could be due to binary motion or pulsation at the period of the LSP. These two possibilities are now discussed.

4.1. Binary members?

Assuming the distribution of radial velocity shifts for non-LSPVs can be represented by the gaussian distribution $n \propto e^{-(v_r')^2/a^2}$, then the curve for $a = 1.3$ fits this distribution fairly well. This is the dotted curve shown in Figure 5. The solid curve in Figure 5 is the result of the following Monte Carlo simulation. The radial velocity distribution (RVD) for LSPVs are considered to be the result of two independent effects. The first is due to stellar pulsation, and is represented by the RVD of the non-LSPVs. The second is due to orbital motion. A random radial velocity shift is drawn from the gaussian RVD of the non-LSPVs. A second random radial velocity shift is calculated from a randomly selected inclination angle, orbital phase angle, reference orbital phase angle and orbital separation (using equation 19 in Han et al. 1995), given an average primary stellar mass and mass-ratio. The orbital phase angle is drawn from a distribution that depends on the orbital period, the length over which the stars were actually observed, in our case about 1 year, and reference orbital phase angle. These two radial velocity shifts are then added. A set of such velocity shifts were calculated for binaries with an average primary mass of $1.5\,M_{\odot}$, an average mass ratio of 0.33, separations greater than $300\,R_{\odot}$, periods shorter than 18 years (the maximum period in the sample is about 18 years) and with the orbital plane within 60° of the line of sight. The resulting velocity shift distribution is the solid curve is Figure 5. This curve fits the RVD of the LSPVs well, showing that the larger radial velocity shifts of the LSPVs can be explained by assuming that these stars are in binary systems.

4.2. Pulsation as the LSP?

To test whether pulsation is a possible explanation for the broader RVD of the LSPVs a second Monte Carlo simulation was performed. Here it is again assumed that the RVD for LSPVs is the result of two independent effects, firstly pulsation at the primary pulsation period and secondly pulsation at the LSP. The first effect was modeled as above. The second effect was modeled as a simple sinusoidal variation in stellar radius.

A random period was drawn from the observed LSP distribution. The LSP distribution can be fairly well approximated by two uniform distributions, one with $2.7 < Log(P) < 3.1$ and the other with $3.1 < Log(P) < 3.6$, with P in days, with 10 of the 28 stars having $Log(P) > 3.1$ (ignoring V Hya in this case). Given a mean LSP pulsation amplitude (difference between minimum and maximum radius), a random pulsation phase and random reference pulsation phase a velocity shift can be calculated. Again the pulsation phase is drawn from a distribution that depends on the orbital period, the length over which the stars were actually observed and the reference pulsation phase. This velocity shift was then combined with the velocity shift drawn from the RVD of the non-LSPVs. Assuming a mean LSP pulsation amplitude of $100\,R_{\odot}$ (roughly equivalent to assuming a velocity amplitude, minimum to maximum, of ~ 4.4 km s^{-1}), a whole set of such of such velocity shifts were generated. The resulting distribution of this set is shown by the dashed line curve in Figure 5. This clearly shows that pulsation at a LSP is also a plausible explanation for the observed RVD of the LSPVs.

Hinkle et al. (2002) analysed the radial velocity variations, in 9 northern LSPVs. They find that in 6 of these LSPVs the radial velocity seem to vary with periods similar to the photometric LSP. However they find that assuming a binary hypothesis, 5 of these systems seem to have very similar "orbital" elements, with the remaining system having the largest uncertainty in its velocity curve. On the basis of this they reject the binary hypothesis and favour pulsation at a so far unknown mode, possibly of the type proposed by Wood (2000b), as a possible explanation for the observed photometric and radial velocity LSP. Both the current study and that by Hinkle et al. (2002) clearly shows that velocity variations, beside those due to normal mode pulsation, are associated with the LSP phenomenon in semi-regulars. The velocity variations associated with the LSP found by Hinkle et al. are in the same range as those shown for the LSPVs in Figure 5.

5. Mid-infrared colours of LSPVs

The suggestion by W99 that LSP minima are caused by obscuration by an orbiting dusty cloud or by periodic dust ejection leads to the possibility of differences in the mid-infrared colours between LSPVs and non-LSPVs: excess dust around the LSPVs would be expected to lead to excess mid-infrared emission. Figure 6 is an IRAS two-colour diagram showing the LSPVs and non-LSPV's with reliable IRAS fluxes. The KS two-sample test gave no significant differences between mid-infrared colours for carbon-rich LSPVs and non-LSPVs. The same result is found for the oxygen-rich LSPVs and non-LSPVs. Also shown in Figure 6 is a sample of RCB stars, taken from Clayton (1996), which have an IRAS counterpart. RCB stars are believed to undergo enhanced dust formation at irregular intervals, leading to the very deep minima observed in their light-curves. This dust is believed to be amorphous carbon (see e.g. Clayton 1996).

In Figure 6, some of the RCB stars lie in the same region as the LSPVs and non-LSPVs. These objects clearly do not have significant detectable excess mid-infrared emission as a result of their dust ejection episodes. However, some RCB stars do show excess mid-infrared emission. The absence of such emission from any of the LSPVs hints that dust may not be prominent in these systems. However, the similarity to some of the RCB stars makes this a rather weak statement. Hinkle et al. (2002) also point out the apparent absence of dust in the 9 northern LSPVs they studied.

An alternative method for determining if the LSPVs have mid-infrared emission from circumstellar dust would be to compare the observed mid-infrared IRAS fluxes with the fluxes expected from a model atmosphere of the LSPV. However, in order to do this, an accurate T_{eff} and normalizing flux (ex. K) at the time of the IRAS observations would be required. Since these quantities are not known for these variable stars, we were unable to use this method to check for excess mid-infrared flux.

6. Summary and Conclusions

High resolution spectra of a sample of semi-regular variables have been analysed for velocity variation. It was found that the distribution of radial velocity variations for LSPVs is significantly broader than that for non-LSPVs, and this difference can be explained either by assuming the LSPVs are in binary systems or pulsating radially with a LSP. In the mean, the LSPVs do not seem to have broader spectral lines than non-LSPVs, suggesting that rotation is not the cause of the LSPs. In fact, a significant fraction of the LSPVs seem to have narrower lines than the non-LSPVs. Fourier analysis of the spectrum of V Hya confirms the result of Barnbaum et al. (1995) that this star has broadened lines but the results suggest that rotation alone is not a good model for explaining the line broadening. IRAS photometry shows no significant difference in mid-infrared colours between LSPVs, non-LSPVs and many RCB stars which are known to be regularly ejecting dust. Hence, no definite conclusion can be drawn from IRAS data as to the presence of dust in LSPVs compared to non-LSPVs.

In summary, the results in this paper favour either binarity or pulsation as the cause of the LSPs in the $\sim$25% of semi-regular variables where they are observed. An ongoing monitoring program is being undertaken to obtain more spectra with good phase coverage. Hopefully, the resulting velocity curves, when compared to light curves and spectra type changes, will allow us to distinguish between these two possibilities.

This research has benefited from use of the SIMBAD database, operated at CDS, Strasbourg, France

REFERENCES

Barnbaum, C., Morris, & M., Kahane, C. 1995, ApJ, 450, 862

Clayton, G. 1996, PASP, 108, 225

Gray, D. F. 1976, The Observation and Analysis of Stellar Photospheres (New York: Wiley)

Han, Z., Eggleton, P. P., Podsiadlowski, P., & Tout, C. A. 1995, MNRAS, 277, 1443

Hinkle, K. H., Lebzelter, T., Joyce, R.R., & Fekel, F. C. 2002, AJ, 123, 1002

Höfner, S., Feuchtinger, M. U., & Dorfi, E. A. 1995, A&A 297, 815

Houk, N. 1963, AJ, 68, 253

Kholopov, P. N. 1985, General Catalogue of Variable Stars (4th ed.; Moscow: Nauka Publishing House) (GCVS)

Kiss, L. L., Szatmáry, K., Cadmus, R. R. Jr., & Mattei, J. A. 1999, A&A, 346, 542

Knapp, G. R., Dobrovolsky, S. I., Ivezić, Z., Young, K., Crosas, M., Mattei, J. A., & Rupen, M. P. 1999, A&A, 351, 97

Olivier, E., Whitelock, P., & Marang, F. 2001, MNRAS, 326, 490

Schwarzschild, M. 1975, ApJ, 195,137

Soker, N., & Clayton, G. C. 1999, MNRAS, 307, 993

van der Veen, W. E. C. J., & Habing, H. J. 1988, A&A, 194, 125

Winters, J. M., Fleischer, A. J., Gauger, A., & Sedlmayr, E. 1994, A&A 290, 623

Wood, P. R., et al. 1999, in IAU Symp. 191, Asymptotic Giant Branch Stars, ed. T. Le Bertre, A. Lébre, & C. Waelkens (Chelsea Michigan:ASP), 151 (W99)

Wood, P. R. 2000a, PASA, 17, 18

Wood, P. R. 2000b, in ASP Conf. Ser. 203, The Impact of Large Scale Surveys on Pulsating Star Research, ed. L. Szabados, & D. W. Kurtz (San Francisco, Calif.: Astronomical Society of the Pacific), 379

NAME	SPEC TYPE	VAR TYPE	P_{puls} (day)	LSP (day)	NAME	SPEC TYPE	VAR TYPE	P_{puls} (day)	LSP (day)
Z Eri	M5III	SRb	80	746	V574 Oph	M4	SRa	72	500
V Eri	M5/M6IV	SRb	97	1209	RT Pav	M4/M5III	SR	85	757
S Lep	M5III	SRb	90	883	EI Del	M2	SRb	20	600
SX Mon	M6.5	SR	100	1100	BM Aqr	M3III	SRb	60	550
CO CMa	M3IIIe	SRb	80	700	W Ori	CII	SRb	212	2450
RT Cnc	M5III	SRb	90	542	RT Ori	CII	SRb	321	3200
SY Vel	M5/M6III	SRb	63	1400	RV Mon	CII	SRb	132	1047
SU Hya	M4III	SRb	95	780	Y Hya	C	SRb	95	1200
BZ Car	M3	SRb	97	1800	V Hya	C	SRa	533	6160 ± 400
T Crt	M6III	SRb	70	1006	T Mus	C	SR	93	1021
AN Vir	M6III	SRb	100	1000	TW Oph	CII	SRb	165	2000
W Nor	M4/M5III	SRa	135	1300	V Pav	C	SRa	225	3735
V521 Oph	M	SRb	320	3500	V Aql	CII	SRb	353	2270

Table 1: The sample of LSPVs. Periods are taken from Houk (1963), except for V Hya whose LSP is taken from Knapp et al. (1999). Spectral types are from *SIMBAD* and variable types are from the GCVS.

NAME	SPEC TYPE	VAR TYPE	P_{puls} (day)	NAME	SPEC TYPE	VAR TYPE	P_{puls} (day)
AG Cet	M5III	SRb	90	V763 Cen	M3III		60
SU Eri	M4III	SRb	112	V Aqr	M6e	SRa	244
RR Eri	M5III	SRb	97	SZ Vel	M5	SRb	150
T Cae	CII	SR	156	CK Car	M3.5	SRc	525
RX Lep	M6III	SRb	60	U Hya	CII	SRb	450
Y Tau	CII	SRb	242	RR Crt	M5	SRb	
GK Ori	N	SR	236	RR Mus	C	SRb	75
RY Mon	N	SRa	456	EV Vir	M3III	SRb	120
GH CMa	M4III	SRb	20	V Nor	M6III	SRb	156
BP Cnc	M3III	SRb	40	V515 Oph	M	SRb	304
GO Vel	M4III	SRb	75	V520 Oph	M	SRd	117
AK Hya	M6III	SRb	75	TY Oph	N	LB	
IN Hya	M3	SRb	65	Y Pav	CII	SRb	233
IO Hya	M4III	SRb	80	SX Pav	M5III	SRb	50
RW Cen	C	SRa		UV Aql	CII	SRa	385

Table 2: The sample of semi-regulars without a LSP. Periods and variable types are taken from the GCVS. Spectral type are from *SIMBAD*, except for V515 Oph and V520 Oph for which spectral types were inferred from the spectra taken in this study.

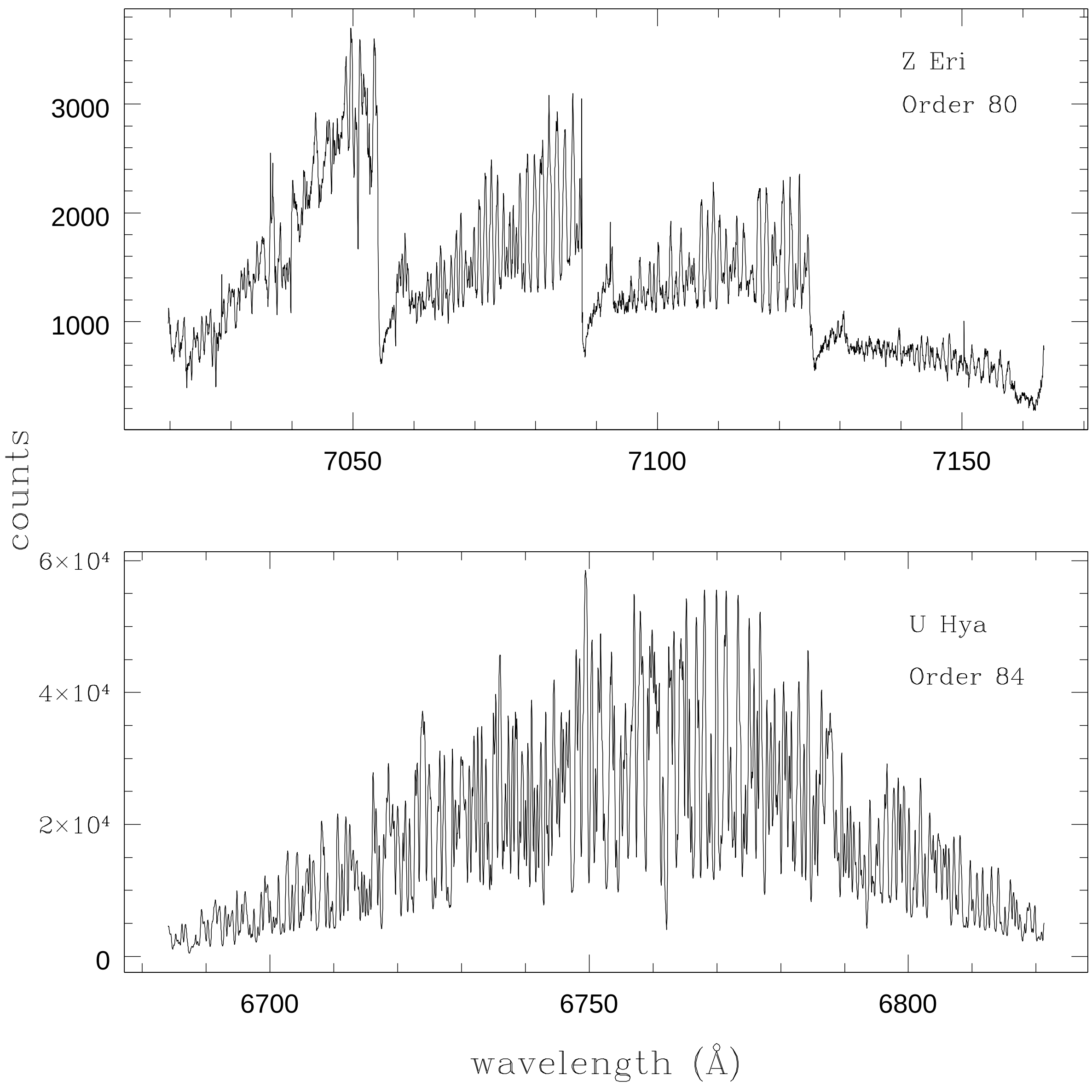

Fig. 1.— Spectra for two variables Z Eri (M-type) and U Hya (C-type). The spectrum of Z Eri clearly show the TiO band heads, which are characteristic of M star spectra. Note that these spectra are not corrected for heliocentric motion.

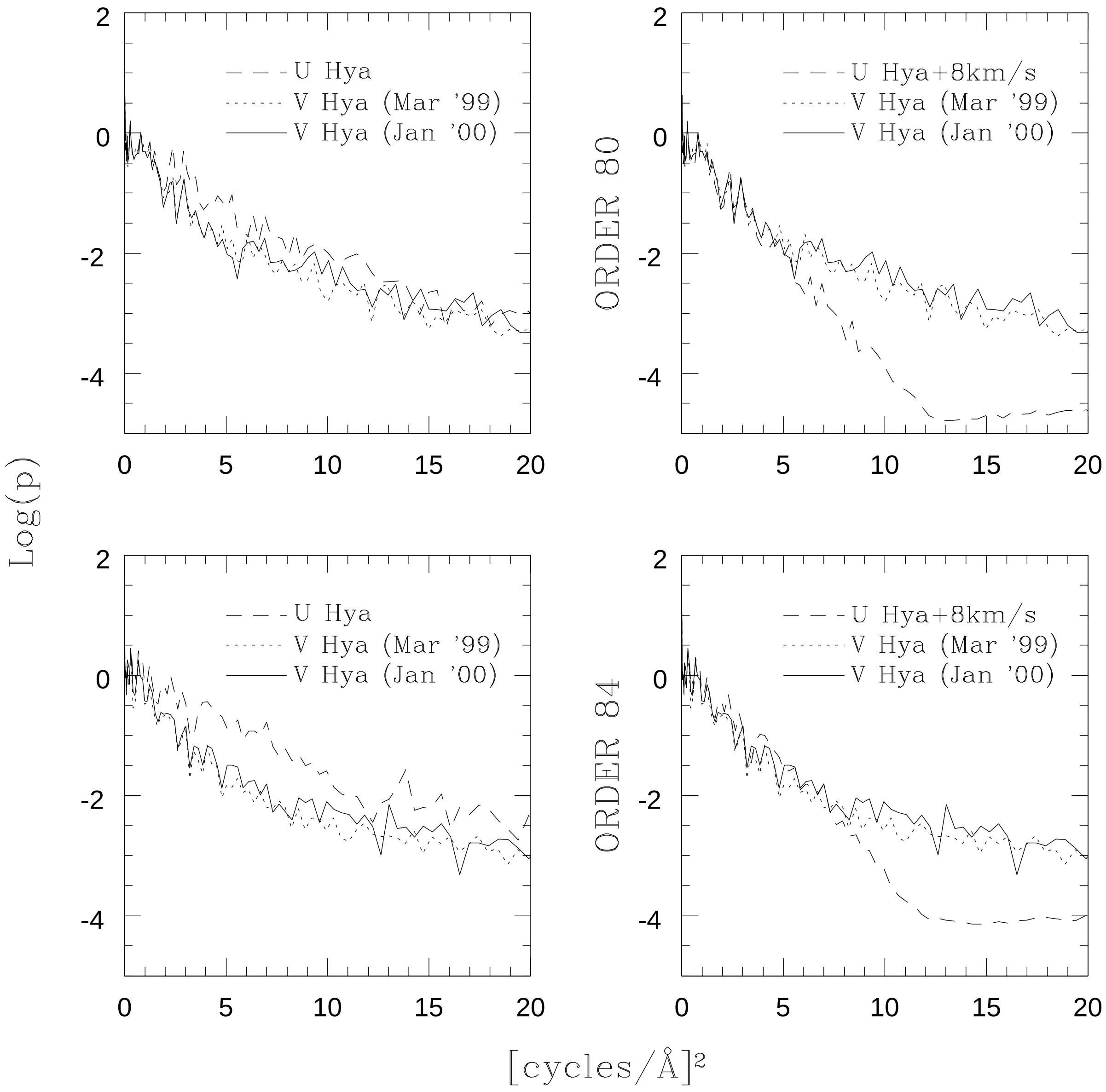

Fig. 2.— Power spectra of the flux spectra of U Hya and V Hya plotted against the square of the frequency. Top and bottom panels are for orders 80 (7030 Å to 7160 Å) and 84 (6700 Å to 6800 Å), respectively. Left panels shows unbroadened spectra of U Hya, and right panels shows rotationally broadened spectra of U Hya with noise of the original power spectrum added. Power spectra are normalized at 0.5 cycles/Å

.

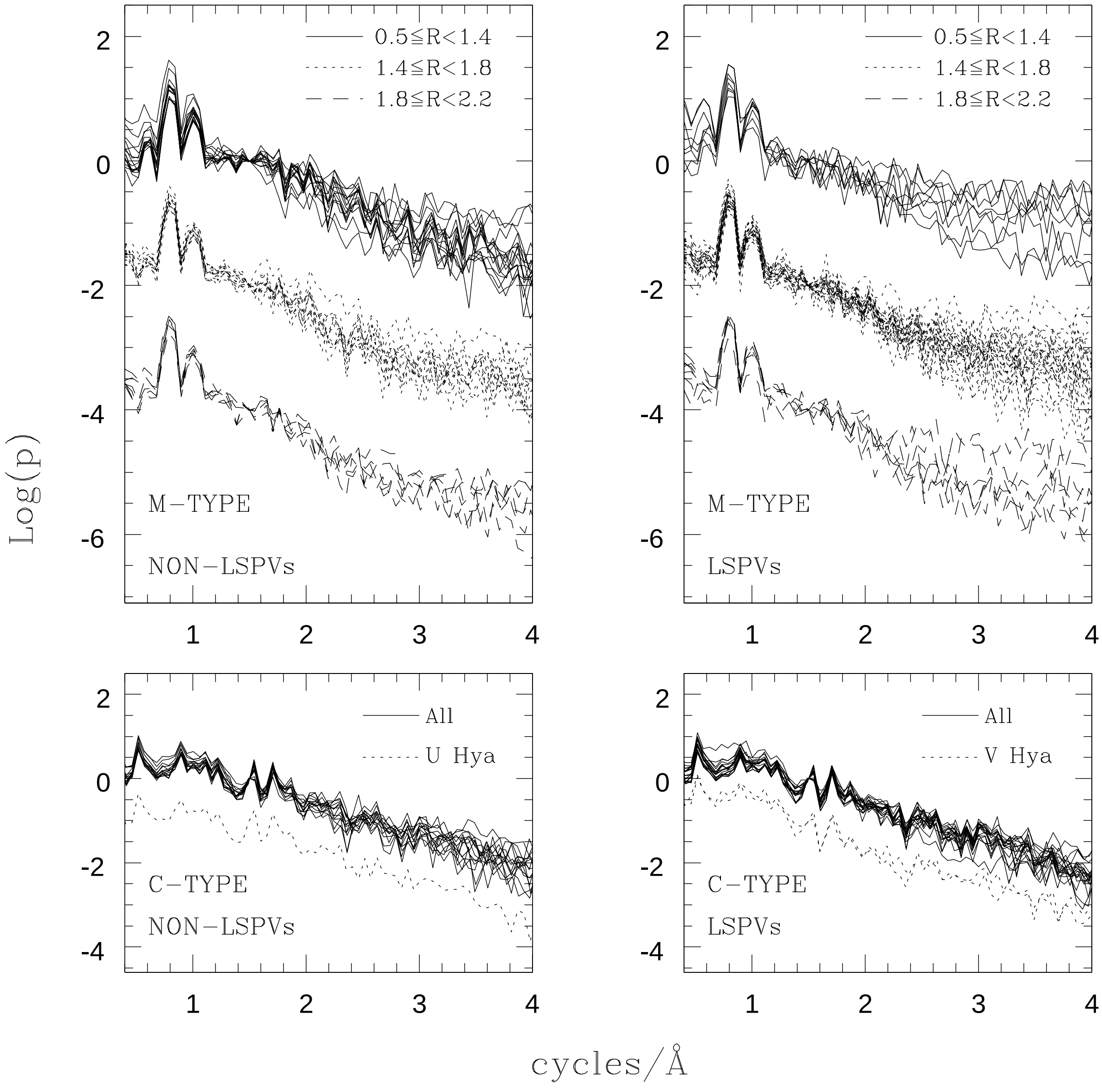

Fig. 3.— Power spectra calculated in the wavelength range 7030 Å to 7160 Å (order 80). Power spectra are normalized at 1.5 cycles/Å. The index R is described in the text.

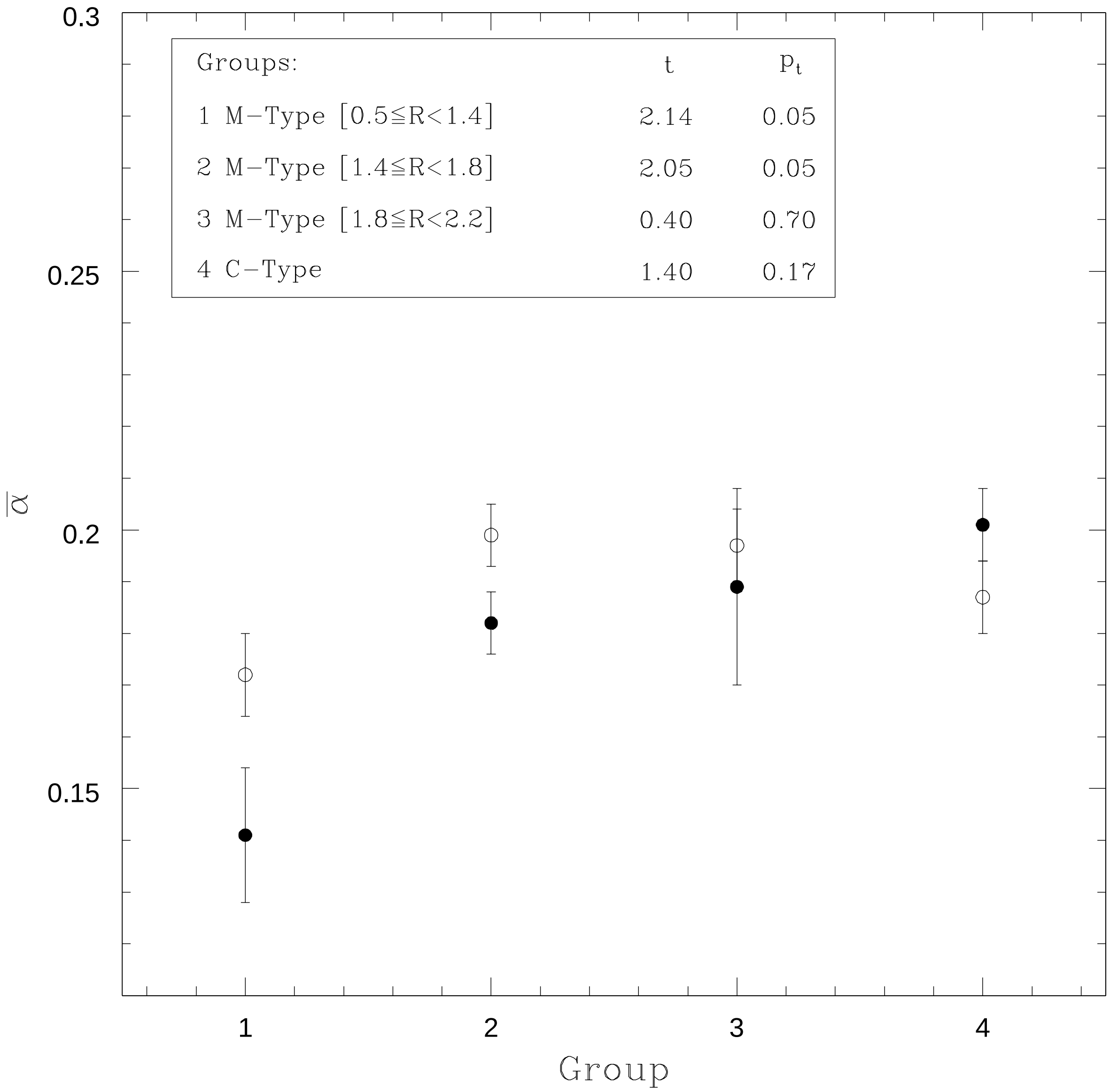

Fig. 4.— The mean value of the slope parameter α for each group. Filled and open symbols refer to LSPVs and non-LSPVs respectively. Error bars shows the standard error in the mean. Inserted panel shows the definition of each group and the t-statistic with its associated significance, p_t, for each group. See text for details.

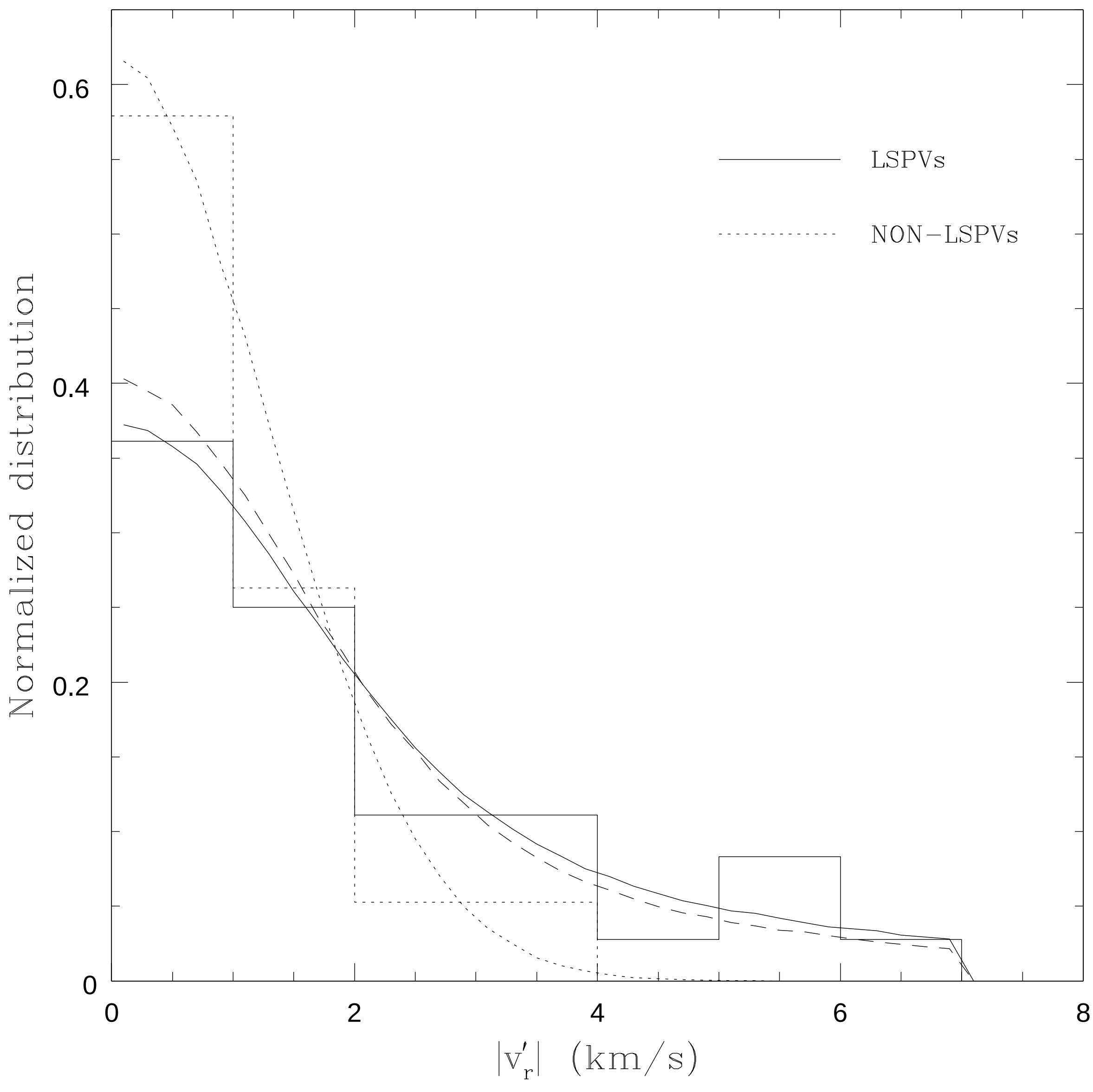

Fig. 5.— Normalized histogram of relative radial velocity (i.e. radial velocity change between two dates) for the 2 groups of stars. Curves are discussed in the text.

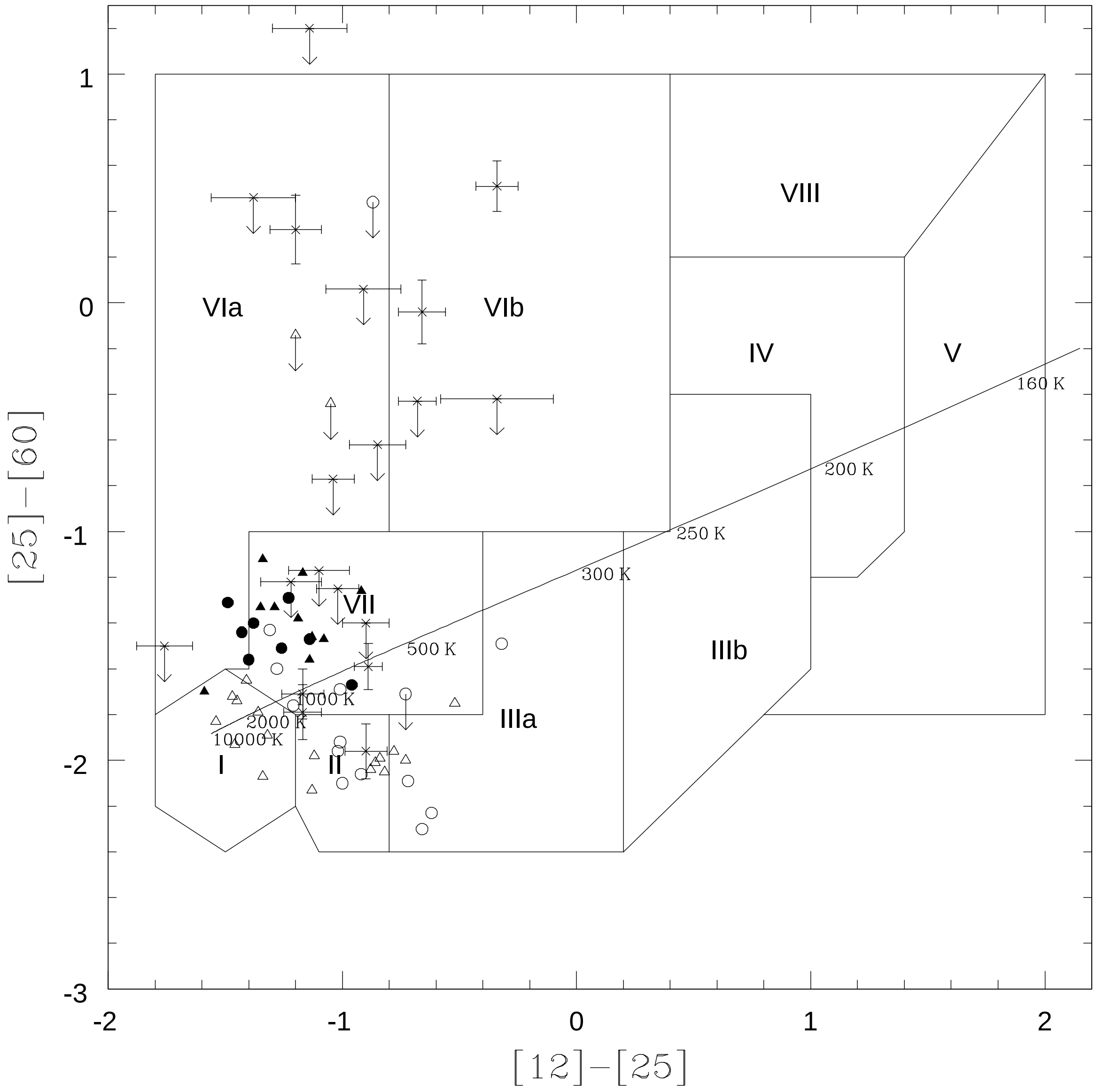

Fig. 6.— The IRAS two-colour diagram. Circles and triangles represent LSPVs and non-LSPVs respectively. The filled and open symbols refer to carbon- and oxygen-rich objects respectively. Crosses represent a sample of RCB stars (see text for details). Objects which have only an upper limit to the 60μm flux are represented by a symbol with an arrow. Colours and regions in the diagram are those defined by Habing & van der Veen (1988). A blackbody line is shown, with temperatures indicated along it.